Food & Function

ROYAL SOCIETY OF CHEMISTRY

PAPER

View Article Online
View Journal | View Issue

Cite this: *Food Funct.*, 2024, **15**, 7577

Edible bird's nest regulates glucose and lipid metabolic disorders *via* the gut–liver axis in obese mice†

Wei Zhang,‡[a,b] Meizhen Zhu,‡[a,b] Xuncai Liu,[c] Maoyao Que,[c] Kelsang Dekyi,[a,b] Linxi Zheng,[a,b] Yichen Zhang,[a,b] Youping Lv,[a,b] Qunyan Fan,*[c] Xinyue Wang*[d,e] and Hongwei Li *[a,b]

Edible bird's nest (EBN) is a traditional food known for its nourishing and functional properties and is found to be involved in anti-oxidation, anti-aging, and anti-influenza mechanisms, immune regulation, and improving cardiovascular diseases, among others. However, the potential of EBN to improve glycolipid metabolism disorders in high-fat-diet induced obesity and the underlying mechanisms remain unexplored. We examined the effects of EBN on glycolipid metabolism in obese mice fed a high-fat diet. Male C57BL/6J mice were fed a high-fat diet for 8 weeks to establish an obesity model. The obese mice were selected and divided into six groups: two model control groups (normal and high-fat diets) and four intervention groups [Neu5Ac and low-, medium-, and high-dose EBN], with 12 mice in each group. After 10 weeks of continuous gavage intervention, only mice in the high-dose EBN intervention group had lower body weight and total fat content, especially visceral fat. Meanwhile, intervention with three doses of EBN reduced serum FBG, TC, LDL, Ox-LDL, IL-1β, IL-6, and TNF-α levels and increased serum HDL levels and energy expenditure. Using the high dosage as a paradigm, EBN intervention increased the sialic acid content in LDL, decreased TMAO in the liver, and increased GLP-1 levels in sera. EBN increased the colonic abundances of *Akkermansia*, *Lactobacillus*, and *Desulfovibrio* and reduced those of *Lysinibacillus* and *Bacillus*. The changes in the microbial community contribute to increasing colonic bile acids, reducing lipopolysaccharide synthesis to protect the intestinal barrier, and lowering inflammation levels. Changes were also observed in colonic transcripts and metabolites and liver gene transcripts and metabolites, which were mainly enriched in pathways of glycolipid metabolism, immune function amelioration, inflammatory signal mitigation, circadian rhythm, bile acid metabolism and insulin resistance. Therefore, EBN may enhance the gut microbiota and intestinal immunity, relieve chronic inflammation levels in serum, improve antioxidant capacity and circadian rhythm in the liver, promote bile acid metabolism, and decrease lipid absorption and lipid synthesis *via* the gut–liver axis. Consequently, this may reduce blood lipid and fat accumulation as well as improve islet function and reduce blood glucose levels.

Received 1st February 2024,
Accepted 11th June 2024

DOI: 10.1039/d4fo00563e

rsc.li/food-function

Introduction

Obesity, defined as abnormal or excessive fat accumulation that impairs health, has become a global epidemic.[1] It is a chronic, relapsing, multifactorial disease accompanied by metabolic disorders and other associated comorbidities (*e.g.*, diabetes mellitus, cardiovascular disease, and cancer), which can severely affect virtually all organ systems, affecting both physical and mental health in a variety of ways.[2] Obesity is now considered as a serious public health issue and is one of the most common non-communicable diseases (NCDs).[1,3] According to the latest estimates, nearly 14% of men and 20% of women in the world's population (more than one billion people) will develop obesity by 2030.[4] Obesity has strong

[a]*State Key Laboratory of Vaccines for Infectious Diseases, Xiang-An Biomedicine Laboratory, School of Public Health, Xiamen University, China. E-mail: rocque@xmu.edu.cn; Fax: +86-0592-2181578; Tel: +86-18905920451*
[b]*State Key Laboratory of Molecular Vaccinology and Molecular Diagnostics, National Innovation Platform for Industry-Education Integration in Vaccine Research, Xiamen University, China*
[c]*Xiamen Yan Palace Seelong Biotechnology Co., Ltd, Xiamen 361100, China. E-mail: 23095216@qq.com*
[d]*Department of Nutrition, Zhongshan Hospital (Xiamen), Fudan University, Xiamen, Fujian Province, China. E-mail: wang.xinyue@zsxmhospital.com*
[e]*Xiamen Clinical Research Center for Cancer Therapy, China*

†Electronic supplementary information (ESI) available. See DOI: https://doi.org/10.1039/d4fo00563e

‡These authors contributed equally to this study.

genetic and environmental features in its pathogenesis, amplifying the influence of genetic susceptibility and environmental factors on disorders of glucolipid metabolism.[2,5] Ectopic expansion of white adipose tissue and excessive accumulation of certain nutrients and metabolites disrupt metabolic homeostasis *via* insulin resistance, dysfunctional autophagy, and the gut microbe–hepatic/brain/pancreatic axis, which further exacerbates systemic inflammation upon immune–metabolism dysregulation, resulting in accelerated loss of β-cell function and gradual elevation of blood glucose levels.[6,7] Abnormal inflammation, fibrosis, hypoxia, dysregulation of adipokine secretion and disruption of mitochondrial function, in turn, exacerbate the condition of white adipose tissue.[8,9] Therefore, interventions aimed at reducing adipose tissue, improving pancreatic islet function, and controlling glucose–lipid metabolism disorders in obese patients are effective measures for preventing the development of diabetes mellitus, coronary heart disease and other diseases.

In recent years, the exploration of foods or food products capable of reducing weight and improving obesity-related glycolipid metabolism has become a focal point in nutritional research.[10] Edible bird's nest (EBN) is a traditional food known for its nourishing and functional properties.[11] EBN has been found to contain bioactive compounds such as 9-*O*-acetylated GD3, glycopeptide, sialic acid, tetraacetyl-thymol-beta-D-glucoside, epidermal growth factor, and glucose-regulated protein,[12,13] which are involved in renoprotection, skin moisturizing, mitochondrial protection, relieving oxidative stress and inflammation, regulating cholesterol-related genes, improving type 2 diabetes, and enhancing male reproduction.[13–15] Ready-to-eat EBN beverages can be analyzed for their EBN content using the active ingredient sialic acid, providing a better estimation of the EBN content.[16] Sialic acid is a general term for a class of nine-carbon sugar compounds whose biological activity has become a new area of research. It is typically modified at the end of the glycan chain of mucopolysaccharides, glycoproteins, or glycolipids in the form of *N*- or *O*-glycosides, serving as an important structural basis for the diversification of the structure and function of carbohydrate complexes.[17] Sialic acid and its derivatives have a wide range of applications in food, medicine and disease diagnosis.[18] *N*-Acetyl neuraminic acid (Neu5Ac), the most widely distributed form of sialic acid, serves as a crucial modification component of glycolipids and glycoprotein terminals on human cell membranes and is associated with human health.[18] Currently, numerous studies have focused on the potential of Neu5Ac to improve obesity-induced disorders of glucose and lipid metabolism. It is speculated that the effects of Neu5Ac on lowering blood lipids may be associated with the activation of lipoprotein lipases, thereby enhancing the hydrolysis of triglycerides and reducing the concentration of cholesterol by accelerating its reverse transport,[19] scavenging reactive oxygen species, and restoring the activity of antioxidant enzymes.[19]

Compared to sialic acid, EBN is a more intricate substance in terms of its composition. It contains not only sialic acid but also other active components such as glycopeptides, which means that EBN has a higher utilization rate than sialic acid alone, potentially making it more effectively utilized by the body. Functionally, EBN has been found to exhibit anti-inflammatory, antioxidant, and cholesterol metabolism-regulating properties.[14] Additionally, it can enhance intestinal flora and safeguard the intestinal mucosa.[20–22] These studies suggest that EBN may effectively combat obesity and carbohydrate metabolism disorders. Nevertheless, there is currently a lack of research on the effects of EBN on improving glycolipid metabolism disorders caused by high-fat diet-induced obesity and the associated mechanisms.

Building upon preliminary research indicating that EBN can enhance cholesterol metabolism, protect mucosal epithelial tissue, and influence the gut microbiota, this study hypothesized that EBN intervention may modulate glucose and lipid metabolism in obese mice *via* the gut–liver axis. Employing a high-fat diet-induced obese mouse model, the study investigates the impact of EBN intervention on glucose and lipid metabolism. By integrating transcriptomic and metabolomic data from both gastrointestinal and hepatic tissues, this study also aims to elucidate the potential mechanisms by which EBN may correct the dysregulation of glucose and lipid metabolism, approached from the perspective of the gut–liver axis.

Materials and methods

Animal experiments

All experimental procedures were conducted in strict accordance with the guidelines outlined by the Institutional Animal Care and Use Committee of the Laboratory Animal Center at Xiamen University and adhered to the principles set forth by the International Association of Veterinary Editors for the Care and Use of Laboratory Animals. The protocols for animal use were thoroughly reviewed and approved by the Animal Ethical and Welfare Committee of the Laboratory Animal Center of Xiamen University (approval no. XMULAC20210010).

The source materials including Neu5Ac [*N*-acetylneuraminic acid, specification: ≥98% (HPLC)] were provided by Wuhan Zhongke Optics Valley Green Biotechnology Co., and EBN (fresh stewed edible bird's nest, containing 0.447 ± 0.019 g of Neu5Ac/100 g) was provided by Xiamen Yan Palace Seelong Biotechnology Co., Ltd. Based on our previous experiences, the success rate of the high-fat feeding obesity model was 40%.[23] Male C57BL/6J mice (n = 180) were purchased from Shanghai Slack Laboratory Animal Co., Ltd and reared at 22 °C with 10%–60% humidity on a 12 h/12 h light–dark cycle with free access to water. After 1 week of adaptive feeding, 12 mice were selected for continued feeding on a normal diet (ND) [Beijing Keao Xieli Feed Co., Ltd; Beijing Feed Certificate (2018) 0673] for 8 weeks. The remaining 168 mice were fed on a high-fat diet [Research Diets, Inc., D12492; Jiangsu Shuangshi Laboratory Animal Feed Department, Su Feed Certificate (2017) 05005] for the same duration, with fat accounting for 60% of the heat energy. Mice that displayed a 40% increase in body weight after feeding on high-fat diets were considered

successful obesity models and were randomly divided into one model control (HFD) and four intervention groups, namely, the Neu5Ac group and the EBN low-dose (EBN_L), EBN medium-dose (EBN_M), and EBN high-dose (EBN_H) groups, with 12 mice in each group. Detailed information on the subgroups can be found in Table 1. Mice were administered the test substance *via* gavage, with the gavage volume set at 0.1 mL/10 g of mouse body weight. Weight and food intake were measured weekly during the 10 weeks of the intervention. Fasting blood glucose (FBG) levels were measured at weeks 0, 4, 6, and 10. At the end of the intervention, the mice's fat mass and lean mass were analyzed using an EchoMRI-100H instrument (EchoMRI International Medical Equipment, Inc.). After fasting for 12 h, the mice were immediately administered a 20% glucose solution by gavage according to their body weight (10 μL g^{-1}).[24] At 0, 30, 60, and 120 min after glucose administration, blood was withdrawn from the tail vein of the mice to measure blood glucose concentrations using a blood glucose meter (Sanuo Biological Sensing Co., Ltd).

Monitoring of animal metabolism

At the end of the intervention, four mice were randomly selected from each group and monitored using the TES PhenoMaster (12-channel) system for 4 days to measure respiratory entropy metabolism and voluntary movement.[25] Each mouse was caged independently. Mice in the ND group were fed a normal diet, whereas those in the other groups were fed a high-fat diet and could eat and drink *ad libitum*. After allowing an initial 48 h period for adaptation, stable metabolic monitoring of each mouse began at 00:00 on the third day and ended at 00:00 on the fourth day, with data recorded at 5 min intervals. The respiratory exchange ratio (RER) and energy expenditure (EE_1) were calculated based on O_2 consumption and CO_2 production measured in the exhaust gas from each cage. Body weight was used to adjust EE_1 values to obtain EE_2 values, and lean body mass was used to further adjust EE_2, thereby deriving the EE_3 values. The EE and RER values were the direct outputs of the instrument, the derivation of which is described in greater detail in ESI S2†, Metabolic Software Calculations Template.

Tissue sampling and index testing

After the 10-week intervention period, the mice were fasted for 12 h. Following inhalation anesthesia with 4% isoflurane (Shenzhen Reward Life Technology Co., Ltd) and euthanasia *via* rapid vertebral dislocation, the eyeballs were removed for blood collection and liver tissues and colons were rapidly collected and rinsed with normal saline. The collected blood was centrifuged at 2000 rpm (382*g*) at 4 °C for 15 min, and the resulting supernatant was collected for measuring biochemical indicators. The liver tissues were rapidly collected, rinsed with normal saline, drained, and weighed. All samples were frozen at −80 °C for later analysis.

Serum was collected using an automatic biochemical analyzer (Minray BS-220) and dedicated supporting kits to determine the levels of total cholesterol (TC), triglycerides (TG), high-density lipoproteins (HDL), and low-density lipoproteins (LDL). Serum was also used to measure serum insulin (INS), IL-1β, IL-6, TNF-α, leptin (LEP), oxidized-LDL (Ox-LDL), and glucagon like peptide-1 (GLP-1) levels, and liver samples were used to measure lipoprotein lipase (LPL) and trimethylamine *N*-oxide (TMAO) levels in mice using respective mouse enzyme-linked immunosorbent assay (ELISA) kits (Shanghai Sanyan Biotechnology Center), according to the manufacturer's instructions.

The insulin resistance index (HOMA-IR) and islet β cell function (HOMA-β) were calculated according to the following formula:

$$\text{HOMA-IR} = \frac{\text{INS}(\text{mUI L}^{-1}) \times \text{FPG}(\text{mmol L}^{-1})}{22.51}$$

$$\text{HOMA-}\beta = \frac{20 \times \text{INS}(\text{mUI L}^{-1})}{\text{PFG}(\text{mmol L}^{-1}) - 3.5}$$

Sialic acid content in LDL (LDL-SIA)

The anticoagulated blood was centrifuged at 1000*g* for 15 min to obtain plasma. The fresh plasma was transferred into a centrifuge tube, adjusted to a density of 1.006 g mL^{-1}, and sealed with nitrogen. After centrifugation at 40 000 rpm for 24 h at 10 °C, the upper layer of the liquid was collected to obtain very low density lipoprotein (VLDL); the lower layer of the liquid was adjusted to 1.063 g mL^{-1} and then centrifuged at 40 000 rpm for 24 h at 10 °C to obtain LDL; the lipoproteins were dialyzed, filled with nitrogen and then sealed for later use.

The LDL sample isolated from the serum was pipetted into a 5 mL centrifuge tube and centrifuged at 4500 rpm for 10 minutes. An equal volume of 10% trichloroacetic acid (TCA)

Table 1 Animal experimental protocol

Group	*N*	Test substance	Supplementation dose in mice (mg d^{-1} kg^{-1})	Gavage concentration (mg mL^{-1})
No supplementation	12	Normal saline	—	—
Neu5Ac	12	*N*-Acetylneuraminic acid	50	5.00
EBN_L	12	Fresh stewed edible bird's nest	2777	27.77
EBN_M	12	Fresh stewed edible bird's nest	5555	55.55
EBN_H	12	Fresh stewed edible bird's nest	11 111[a]	111.11

[a] Calculate the intervention dose of EBN_H based on the Neu5Ac content of 0.447 ± 0.019 g per 100 g in EBN, so that the Neu5Ac content in the intervention dose matches that of the Neu5Ac intervention group. The supplementation dose of the EBN_M group was 0.5 times that of the EBN_L group, and the supplementation dose of the EBN_L group was 0.5 times that of the EBN_M group.

was added and the sample was mixed well and left for 10 minutes at 4 °C. Subsequently, the mixture was left for an additional 10 minutes and then centrifuged at 4500 rpm for another 10 minutes. The resulting supernatant was transferred to a new tube. Cold 5% TCA was added to the precipitate and mixed well. The mixture was centrifuged again at 4500 rpm for 10 minutes and the two supernatants were combined. After adding 2.5 mL of 0.1 moL L^{-1} sulfuric acid, the sample was placed in a water bath at 80 °C for 2 hours and then removed and cooled down before filtering. Next, 0.1 mL of the above liquid was accurately pipetted, followed by the addition of 0.1 mL of 10 mg mL^{-1} *o*-phenylenediamine hydrochloride dissolved in 0.2 mol L^{-1} Na_2HSO_4 and incubation in an 80 °C water bath for 40 minutes. Then, the sample was removed, cooled down, and then filtered through a 0.22 microporous filter membrane. High-performance liquid chromatography (HPLC) was employed to measure the sialic acid content in the LDL samples using the following mass spectrometry conditions: C18 column (Waters Symmetry 250 × 4.6 mm; 5 μm); detector: VWD; column temperature: 35 °C; wavelength: 230 nm; mobile phase: 5% (v/v) methanol containing 4 mmoL L^{-1} ammonium formate and 0.1% (v/v) formic acid, eluting linearly; flow rate: 1 mL min^{-1}; sample volume: 20 μL; mobile phase: acetonitrile : water = 10 : 90.

Oil red O staining (Oil-red) of the liver and hematoxylin–eosin (H&E) staining of the heart

The heart tissue samples were fixed using 4% paraformaldehyde, embedded in paraffin, and cut into sections. Oil red O staining was performed using a modified Oil Red O staining kit (Solarbio Life Sciences, Beijing, China), following the instructions provided by the manufacturer. Hematoxylin–eosin (H&E) staining was performed using an H&E staining kit (Solarbio), and the stained sections were assessed *via* microscopy (Leica-DM4B; Leica, Wetzlar, Germany).

16S rDNA sequencing

Colon contents were swiftly frozen in liquid nitrogen post-sampling and stored at −80 °C. DNA was extracted from these samples using the HiPure Stool DNA kit (Magen, Guangzhou, China). The conserved 16S rDNA gene region (V3: 341F, CCTACGGGNGGCWGCAG; V4: 806F, GGACTACHVGGGTATCTAAT) was polymerase chain reaction (PCR)-amplified using suitable primers with barcodes. The resulting amplicons were purified, quantified, and subjected to equimolar pooling for paired-end sequencing (PE250) on an Illumina sequencer (Life Technologies, CA, USA). Raw reads were filtered, assembled, and processed using FASTP (v. 0.18.0). Clean tags were clustered into operational taxonomic units (OTUs) with a ≥97% similarity threshold using the UPARSE pipeline (v. 9.2.64). Chimeric tags were removed using the UCHIME algorithm, and the remaining tags underwent downstream analyses. The most abundant sequence in each OTU served as a representative sequence. Following OTU determination, the gut microbiota indices (community composition, alpha diversity, beta diversity, indicator species, and intestinal flora function) were assessed using the Omicsmart platform (Gene Denovo Biotechnology Co., Ltd Guangzhou, China; **https://www.omicsmart.com**).

Hepatic transcriptomic analysis

Total RNA was extracted using the TRIzol reagent kit (Invitrogen, Carlsbad, CA, USA) following the manufacturer's protocol. The RNA quality was assessed using an Agilent 2100 bioanalyzer (Agilent Technologies, Palo Alto, CA, USA) and verified by RNase-free agarose gel electrophoresis. After total RNA extraction, eukaryotic mRNA was enriched using oligo(dT) beads. The enriched mRNA was fragmented into short fragments using fragmentation buffer and reverse-transcribed into cDNA using the NEB Next Ultra RNA Library Prep Kit for Illumina (NEB #7530, New England Biolabs, Ipswich, MA, USA). The purified double-stranded cDNA fragments were subjected to end repair, A tailing, and ligation with Illumina sequencing adapters. The ligated sequences were purified using AMPure XP beads (1.0×) and subsequently amplified by PCR. The resulting cDNA library was sequenced by Gene Denovo Biotechnology Co. (Guangzhou, China) using an Illumina Novaseq6000 sequencer.

Metabolomics analysis of the colon and liver

Mouse tissue samples were preprocessed according to a previously described method.[26] Ultra-high-performance liquid chromatography-tandem mass spectrometry (UHPLC-MS/MS) analyses were performed by Gene Denovo Co., Ltd (Guangzhou, China) using a Vanquish UHPLC system (Thermosphere, Germany) coupled with an Orbitrap Q ExactiveTM HF-X mass spectrometer (Thermo Fisher, Germany). The raw data files generated using UHPLC-MS/MS were processed using Compound Discoverer 3.1 (CD 3.1; Thermo Fisher Scientific) to perform peak alignment, peak picking, and quantitation for each metabolite. Normalized data were used to predict the molecular formulae based on additive ions, molecular ion peaks, and fragment ions. To obtain accurate qualitative and relative quantitative results, the detected peaks were matched to the spectra in the mzCloud (**https://www.mzcloud.org/**), mz Vault, and MassList databases.

Quantitative real-time PCR

Total RNA was isolated from cells or tissues using the TRIzol method (Invitrogen TRIzol, cat#15596026). First-strand cDNA was synthesized using a cDNA synthesis kit (Thermo Fisher Scientific™, cat# K1641). Quantitative PCR was performed using the Fast SYBR™ Green Master Mix (Applied Biosystems™, cat# 4385610). The results were analyzed on an ABI StepOnePlus real-time PCR system (Applied Biosystems, USA, RRID: SCR_015805), using the $2 - \Delta\Delta Ct$ method as described previously.[27] Primers were designed using Primer Premier 5, were synthesized by Genecreate Biotech (Wuhan, China), and are listed in Table S1†. GAPDH was used as a loading control, and mRNA levels were normalized relative to *GAPDH* levels.

Statistical analysis

Data were analyzed using SPSS 22.0 and R statistical software. Repeated measures data were analyzed for variance using multivariate analysis. For normally distributed data with homogeneous variance, a one-way analysis of variance (one-way ANOVA) was used to compare differences between groups, and Fisher's least significant difference method (LSD) was used for pairwise comparisons between groups. In the case of normally distributed data for which the variance was non-homogeneous, we used Dunnett's *T*3 test for pairwise comparisons between the groups. For non-normally distributed data, we used the non-parametric Kruskal–Wallis *H* test for comparison between groups, and the Nemenyi method was used for pairwise comparison of the overall means between groups. Differences were considered significant at the $a = 0.05$ level.

Results

Weight and fat distribution

As shown in Fig. 1(A), the EBN intervention demonstrates a dose–effect relationship in reducing weight in obese mice. The high-dose EBN intervention displayed the most effective weight control and surpassed the effects of Neu5Ac intervention. At the beginning of the intervention, there was no significant difference in body weight between the various test substance groups and the HFD group mice ($P < 0.05$). By the end of the 10-week intervention, the high-dose EBN intervention could reduce the weight of the mice (38.09 ± 4.41 g *vs.* HFD 41.88 ± 3.79 g, $P < 0.05$). However, the other intervention groups did not show any weight reduction ($P > 0.05$). As shown in Fig. 1(B and C), the high-dose EBN intervention could reduce fat mass (9.80 ± 3.60 g *vs.* HFD 13.54 ± 2.63 g, $P < 0.05$), while other intervention groups did not reduce fat mass ($P > 0.05$). As shown in Fig. 1(D and E), both medium- and high-dose EBN interventions reduced liver weight ($P < 0.05$). Additionally, EBN intervention could effectively diminish liver lipid accumulation, with a notable improvement in the corresponding liver tissue structure. Moreover, a dose–response relationship was observed in EBN intervention groups, with the high-dose EBN intervention yielding the most optimal outcomes. The Neu5Ac intervention exhibited a similar effect to the medium-dose EBN intervention but was less effective compared to the high-dose EBN intervention.

Core glycolipid biomarkers and proinflammatory cytokines in the serum and liver

As shown in Fig. 2(A), each dose of EBN intervention reduced the FBG levels in obese mice ($P < 0.05$); however, no significant differences were observed between the dosage groups ($P > 0.05$). Nevertheless, the Neu5Ac intervention did not reduce FBG levels ($P > 0.05$) and resulted in higher FBG levels than those observed in the medium- and high-dosage EBN intervention groups ($P < 0.05$). As depicted in Fig. 2(B–E), EBN and Neu5Ac interventions slightly enhanced glucose tolerance in obese mice, but reduced serum INS levels and the HOMA-IR value (all, $P < 0.05$). The high-dose EBN intervention resulted in lower INS levels and HOMA-IR values than the Neu5Ac intervention ($P < 0.05$).

As shown in Fig. 2(F–K), both EBN and Neu5Ac interventions decreased serum TG, TC, LDL, Ox-LDL, L-1β, IL-6, and TNF-α levels and increased serum HDL and the sialic acid load on LDL in serum (all, $P < 0.05$). No dosage-dependent effect was observed in EBN intervention groups. As shown in Fig. 2

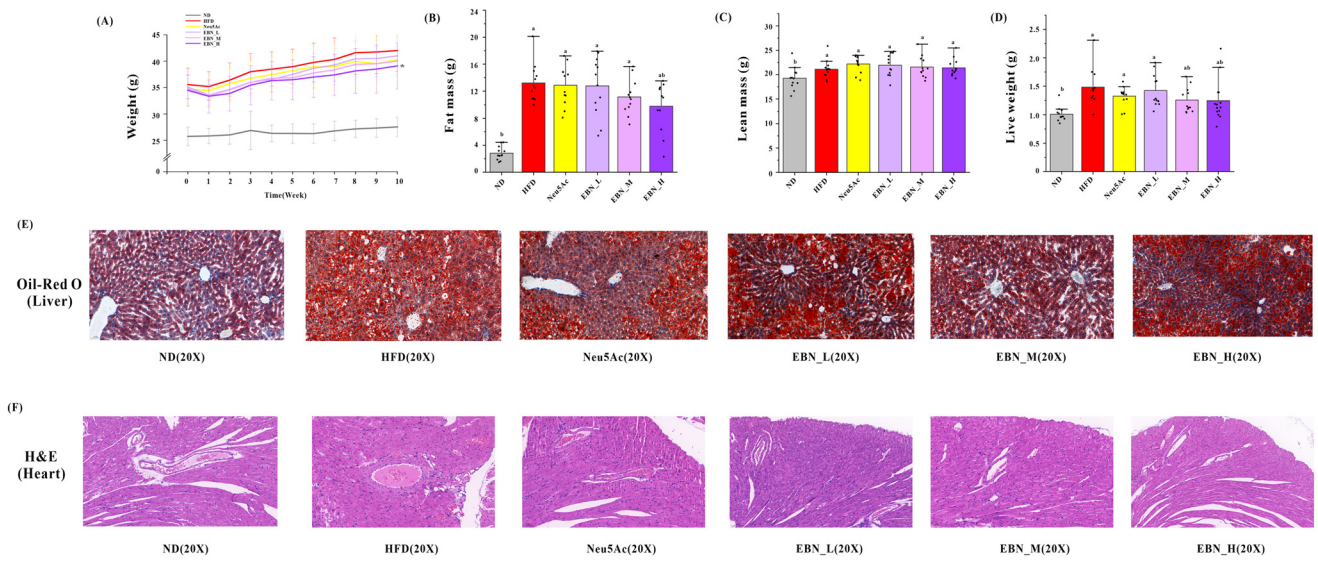

Fig. 1 Changes in the metabolic homeostasis of body mass distribution in obese mice after 10 weeks of EBN intervention. (A) Weight changes from 0 to 10 weeks; (B) fat mass; (C) lean mass; (D) liver weight; (E) liver sections stained with Oil red O; (F) heart sections stained with hematoxylin and eosin; a: $P < 0.05$, compared with the normal diet (ND) group. b: $P < 0.05$, compared with the high-fat diet (HFD) group. All values are mean ± SD ($n = 12$).

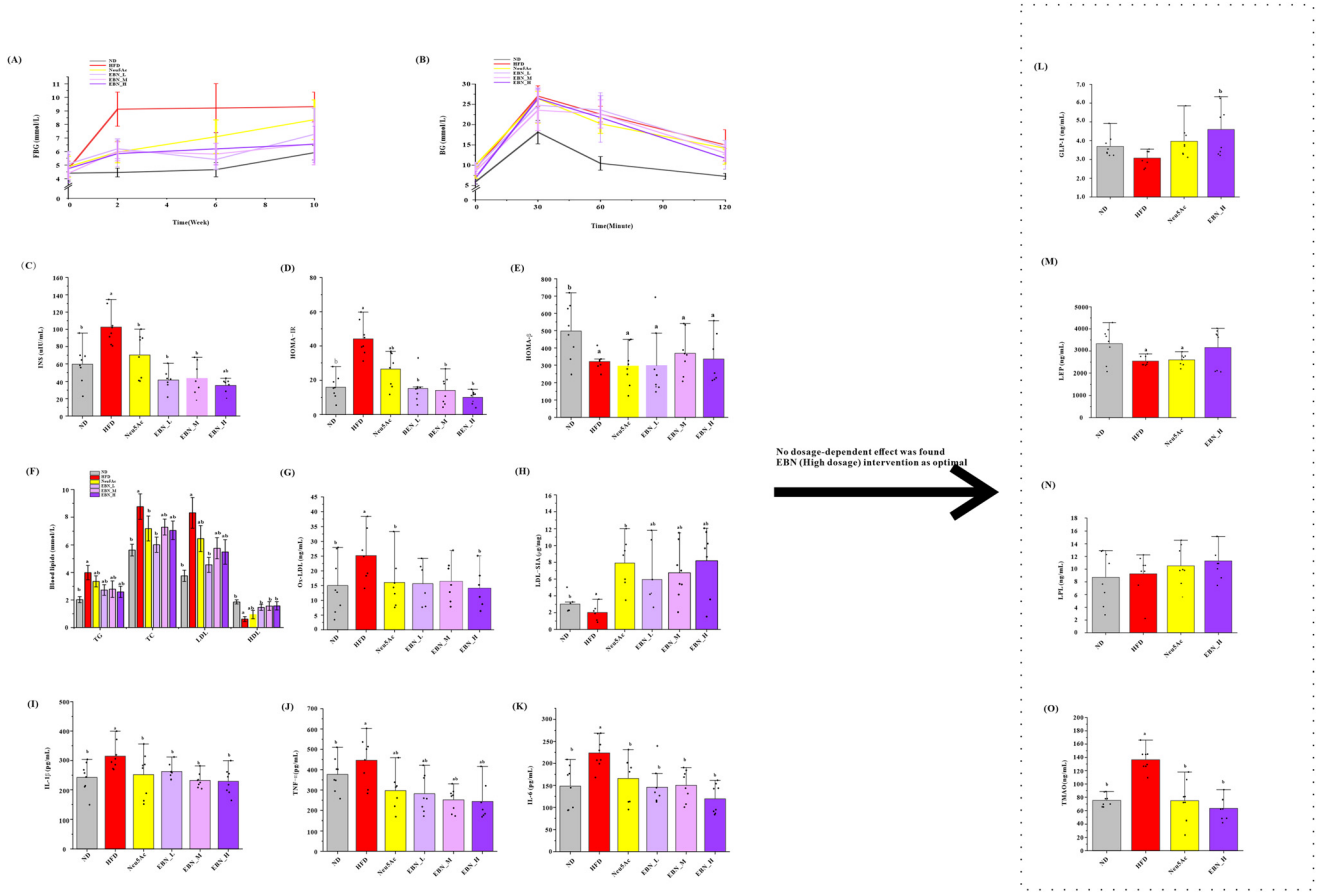

Fig. 2 Changes in the metabolic homeostasis of glucolipid biomarkers and core inflammatory cytokines in obese mice after 10 weeks of EBN intervention. (A–E) Changes in blood glucose levels and glucose regulation ability: (A) changes in fasting blood glucose levels at weeks 0, 3, 6, and 10; (B) oral glucose tolerance test (OGTT); (C) insulin in sera; (D) insulin resistance index (HOMA-IR); and (E) insulin cell function index (HOMA-β). (F–M) Changes in blood lipids: (F) blood lipids including total cholesterol (TC), triglyceride (TG), low-density lipoprotein cholesterol (LDL), and high-density lipoprotein cholesterol (HDL); (G) oxidized low-density lipoprotein cholesterol (Ox-LDL); (H) sialic acid conjugated to LDL (LDL-SIA) level; (I–K) changes in inflammation factor levels in sera: (I) IL-1β; (J) TNF-α; and (K) IL-6; and (L–O) using high-dose EBN as the paradigm: (L) glucagon-like peptide-1(GLP-1) in serum; (M) leptin (LEP) in serum; (N) lipoprotein lipase (LPL) in the liver; and (O) trimethylamine oxide (TMAO) in the liver. a: $P < 0.05$, compared with ND. b: $P < 0.05$, compared with HFD. All values are mean ± SD ($n = 8$).

(L–O), using the high-dose EBN intervention as a paradigm, the EBN intervention increased GLP-1 in the serum ($P < 0.05$), whereas Neu5Ac did not ($P > 0.05$). Both EBN and Neu5Ac interventions reduced TMAO levels in the liver ($P < 0.05$).

2-Day energy metabolism monitoring

As shown in Fig. 3, a series of energy metabolism variables, including EE_1, EE_2, EE_3, RER, and the amount of exercise showed no dosage-dependent effects among the three EBN intervention groups (all, $P > 0.05$). Compared to the Neu5Ac intervention group, which paradoxically decreased the energy metabolism variables, the EBN intervention group significantly increased the EE_1, EE_2, and EE_3 values at all dosages with a notable trend ($P < 0.05$).

Colonic microbiota in obese mice

Using the high-dose EBN intervention as a paradigm, beta diversity analysis revealed a distinction in the OTUs of the colonic microbiota between mice in the EBN intervention group and those in the HFD group. Concurrently, using the permutational multivariate analysis of variance test, the results showed $R^2 = 0.403$ and $P = 0.001$, indicating statistically significant differences in the gut microbiota among the groups. This suggests that the EBN intervention is capable of altering the gut microbiota in obese mice (Fig. 4A). At the phylum level, the abundances of *Firmicutes* and *Cyanobacteria* were increased, while the abundance of *Proteobacteria* was decreased in the gut microbiota of obese mice treated with EBN intervention (Fig. 4B). At the genus level, the abundances of *Desulfovibrio*, *Akkermansia*, *Lactobacillus*, and *Solibacillus* were increased, while those of *Enterobacter*, *Lysinibacillus*, *Bacillus* and *Enterococcus* were decreased in obese mice treated with EBN intervention (Fig. 4C). Intestinal flora function analysis indicated that several pathways related to metabolic homeostasis, including carbohydrate metabolism, amino acid metabolism, lipid metabolism, energy metabolism, immune

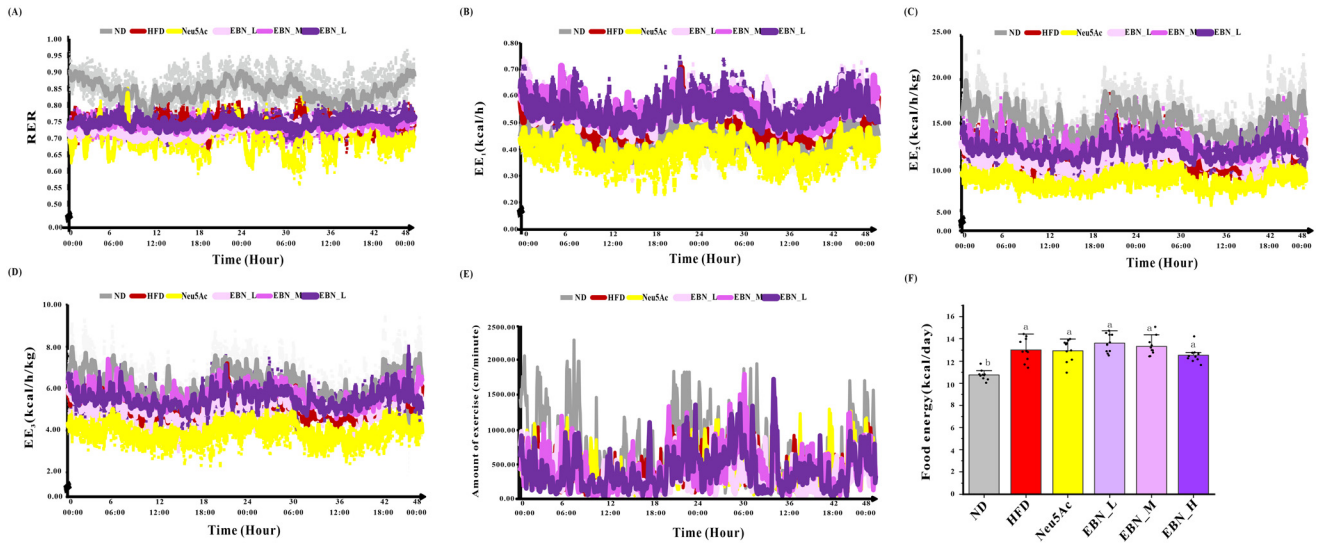

Fig. 3 Changes in the metabolic homeostasis of energy monitoring variables in obese mice after 10 weeks of EBN intervention. (A–C) Energy expenditure: (A) EE_1 (no adjust); (B) EE_2 (EE_1 adjust weight); and (C) EE_3 (EE_2 adjust lean mass); (D) respiratory exchange rate (RER); (E) amount of exercise; (F) food energy (average weekly food consumption per group per individual). a: $P < 0.05$, compared with ND. b: $P < 0.05$, compared with HFD. All values are mean ± SD ($n = 4$).

system, cell growth and death, and preventing infectious diseases, were significantly altered during the 10-week EBN intervention period, affecting gut microbiota-associated functions (Fig. 4D and E). The serum level of GLP-1 was positively related to *Desulfovibrio* abundance, the serum level of IL-1β was positively related to *Lysinibacillus* abundance, and the serum level of IL-6 was positively related to *Bacillus* abundance (Fig. 4F).

Transcriptomes of the autopsied livers and colons of obese mice

Using high-dose EBN intervention as a paradigm, the transcriptome of the colonic mucosa of obese mice was notably changed after 10 weeks of high-dose EBN intervention (Fig. 5A and B). The top 20 pathways that were enriched in the differentially expressed genes are shown in Fig. 5C, substantially impacting functions related to insulin signaling, immunity, cholesterol metabolism, and bile secretion, and the corresponding differentially expressed genes are shown in Fig. 5D. After 10 weeks of Neu5Ac intervention, a slight alteration in the transcriptome was observed in the colonic mucosa autopsied from obese mice (Fig. 5A and B). Six genes associated with insulin signaling (*Ppara*), immunity (*Tlr2*), cholesterol metabolism *(Lrp1*), and bile secretion (*Fxr*, *Tsgr5*, and *Slc102*) were validated using quantitative real-time PCR (Fig. 5I). Compared to the HFD group, the EBN intervention decreased the expression levels of *Ppara*, *Tlr2*, *Lrp1*, and *Slc102* and increased the expression levels of *Fxr* and *Tsgr5* in the colon (all, $P < 0.05$).

The transcriptome of the hepatic tissue from obese mice was remarkably changed after 10 weeks of high-dose EBN intervention (Fig. 5E and F). The top 20 pathways enriched in the DEGs are shown in Fig. 5G. These differentially expressed genes generally function to transduce signaling related to circadian rhythm, glycosphingolipid biosynthesis, protein and fat digestion and absorption and bile secretion, and the corresponding differentially expressed genes are shown in Fig. 5H. Six differentially expressed genes associated with the circadian rhythm (*Per2* and *Bhlhe41*), glycosphingolipid biosynthesis (*Mgat4c*), biosynthesis of unsaturated fatty acids (*Elovl3*), metabolism of trimethylamine (*Fmo3*), and bile secretion (*Slc51a*) were validated using quantitative real-time PCR (Fig. 5I). Compared to the HFD group, EBN intervention decreased the expression levels of *Elovl3* and *Fmo3* and increased the expression levels of *Per2*, *Bhlhe41*, *Mgat4c*, and *Slc51a* in the liver (all, $P < 0.05$).

Metabolome of autopsied liver and colonic contents

As shown in Fig. 6(A–D), using the high-dose EBN intervention as a paradigm, five distinct categories of metabolites in the liver and colonic contents were identified: fatty acids, bile acids, amino acids, carbohydrates, and neurotransmitters. These findings indicated that the EBN intervention had the most pronounced effect on the levels of fatty acids, bile acids, and amino acids. Among the metabolic pathways of differential metabolites in both liver and colonic contents, the top 5 functional pathways identified in the Kyoto Encyclopedia of Genes and Genomes (KEGG) database included the synthesis of fatty acids, the synthesis of bile acids, and the digestion and absorption of proteins. Moreover, an increase in the diversity and quantity of long-chain fatty acids and secondary bile acids was observed in the colonic content, whereas the liver showed a decrease in long-chain fatty acids and primary bile acids, with an increase in conjugated bile acids, which are more conducive to bile acid excretion. It was also found that the levels

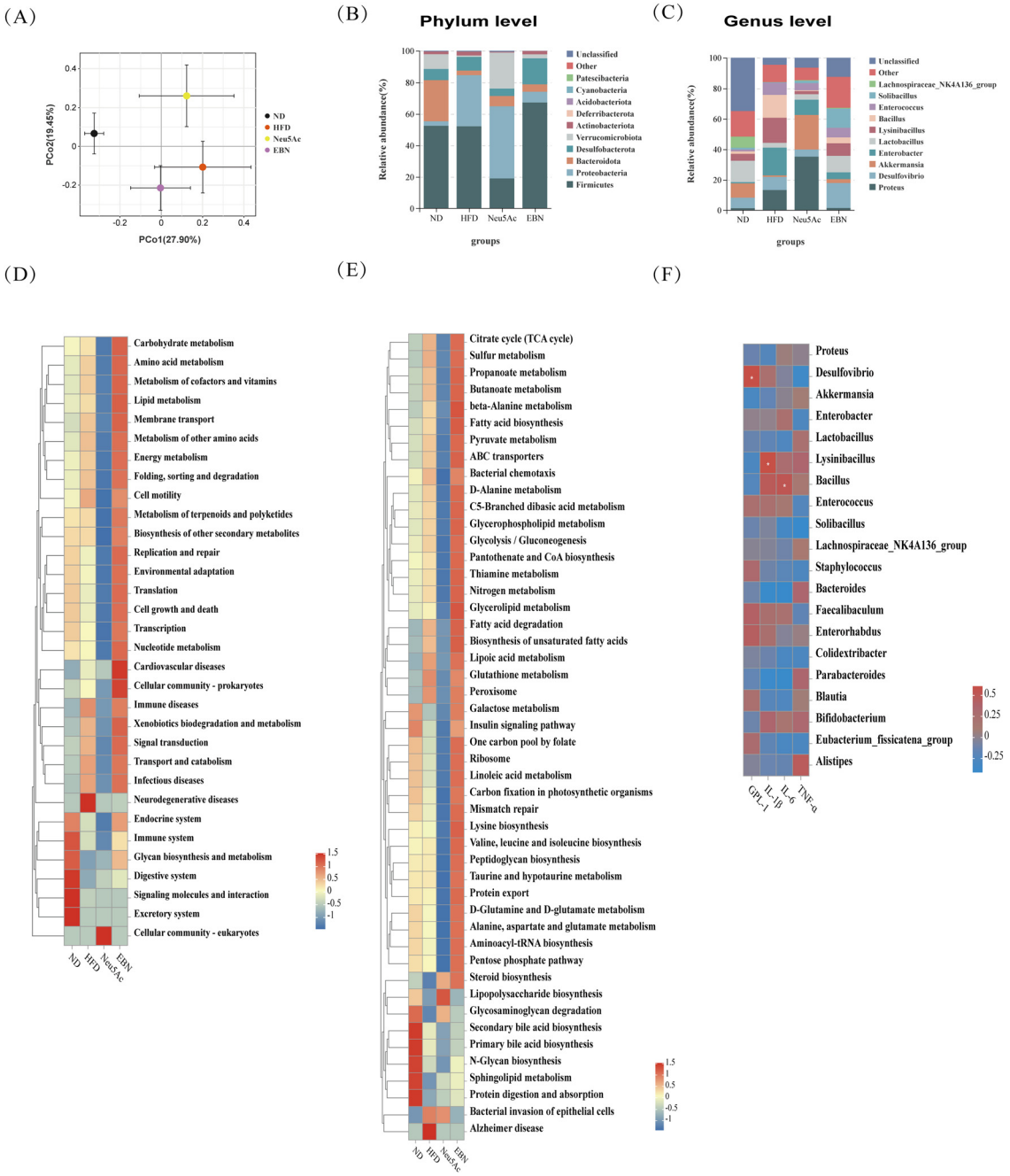

Fig. 4 Changes in the gut microbiota in obese mice after 10 weeks of EBN intervention. (A–C) Species composition and diversity: (A) beta analysis of intestinal flora at the level of operational taxonomic units (OUTs) (P = 0.001, using the permutational multivariate analysis of variance test); (B) relative abundance at the phylum level; and (C) relative abundance at the genus level; (D and E) functional analysis of the intestinal flora: (D) B-class classification function of colonic flora based on the reference sequence of PICRUSt2 and (E) C-class classification function of colonic flora based on the reference sequence of PICRUSt2; and (F) heatmap of the correlation between the intestinal microbiota and serum IL-1, IL-6, TNF-α, and GLP-1 levels. *P < 0.05. N = 4 mice per group.

of monosaccharides and disaccharides (such as glucose, maltose, melibiose, and galactose) decreased in the liver, whereas the polysaccharide content (such as 2′-fucosyllactose and 6′-sialyllactose) increased, suggesting an enhanced ability of the liver to utilize sugar under the EBN intervention.

As shown in Fig. 6(E and F), the correlation analysis between the gut microbiome and metabolome revealed that the abundances of *Desulfovibrio*, *Lysinibacillus*, and *Solibacillus* were positively correlated with bile acids (BAs) and negatively correlated with fatty acids. Additionally, *Lactobacillus* and *Akkermansia* abundances were negatively correlated with fatty acids. It has been hypothesized that an increase in the levels of colonic BAs and fatty acids in mice under the EBN intervention is related to changes in the gut

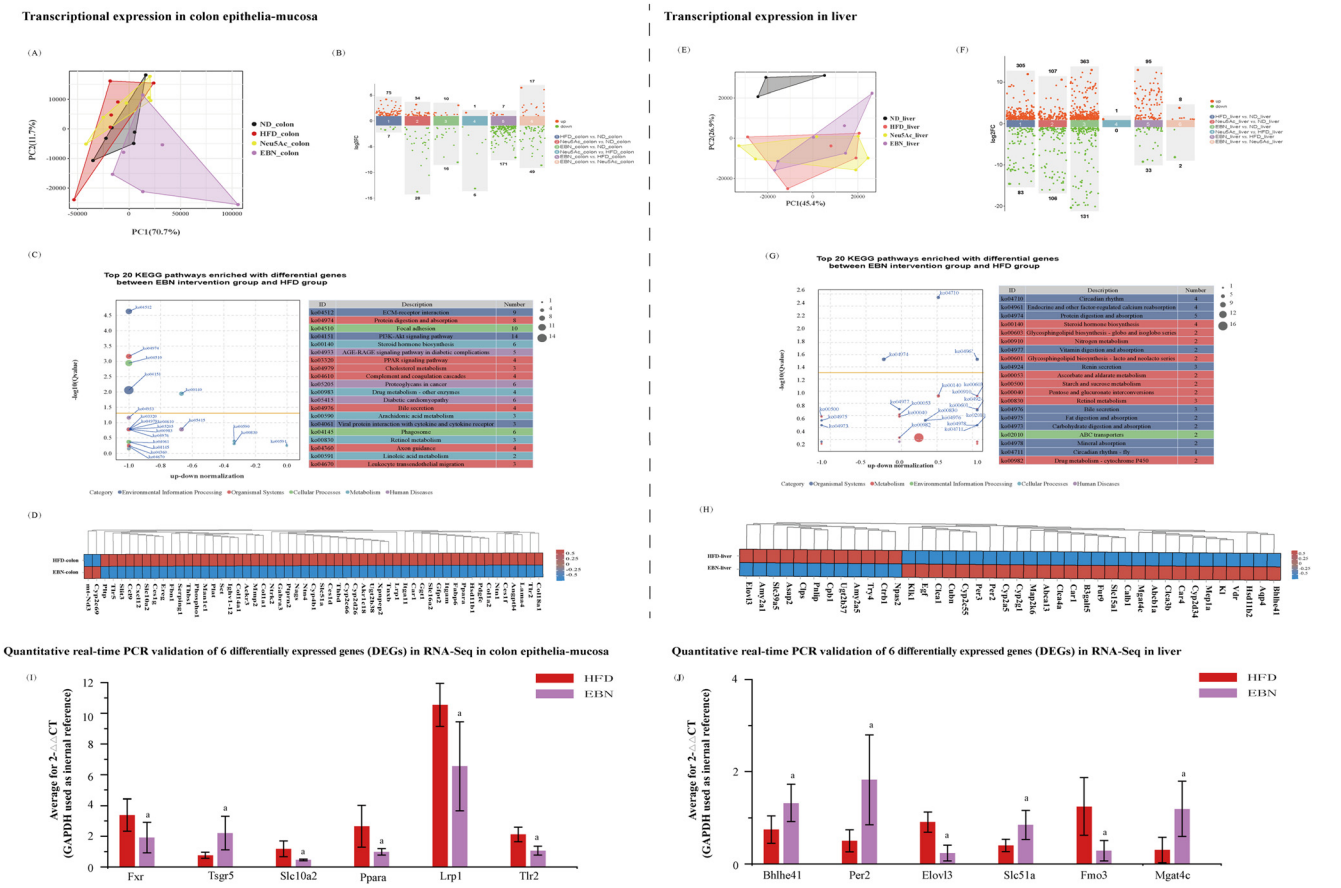

Fig. 5 Changes in transcriptional expression in colon epithelia-mucosa and liver autopsied from 6 obese mice intervened by EBN post 10-week supplementation. (A and B) Transcriptional expression differences in colon epithelia-mucosa: (A) principal component analysis (PCA) of group sample relationships and (B) scatterplot of multiple group differences in transcript expression levels. (C and D) Functional analysis of differential transcriptional expression in colon epithelia-mucosa (EBN *vs.* HFD groups): (C) top 20 Kyoto Encyclopedia of Genes and Genomes (KEGG) pathways enriched with differential transcript expression between the EBN group and the HFD group and (D) differential transcriptional expression of colon genes corresponding to the top 20 differential pathways (EBN *vs.* HFD groups). (E and F) Transcriptional expression differences in the liver: (E) PCA analysis of group sample relationships and (F) scatterplot of multiple group differences in transcript expression. (G and H) Functional analysis of differential transcriptional expression in the liver (EBN *vs.* HFD groups): (G) top 20 KEGG pathways enriched with differential transcriptional expression between the EBN and HFD groups and (H) differential transcriptional expression of liver genes corresponding to the top 20 differential pathways (EBN *vs.* HFD groups). (I) Quantitative real-time PCR validation of 6 differentially expressed genes in the colon. (J) Quantitative real-time PCR validation of 6 differentially expressed genes in the liver; a: $P < 0.05$, compared with the HFD group.

microbiota. The analysis of the relationship between fatty acids and BAs in the liver found that fatty acids were positively correlated with BAs. This indicated that the reduction in dehydrocholic acid and glycocholic acid levels in the liver due to the EBN intervention was associated with a decrease in lipids in the liver. This study also found that aromatic amino acids (AAAs) such as phenylalanine and tryptophan decreased in the liver, while branched-chain amino acids (BCAAs) including isoleucine and valine increased under the EBN intervention. Combining the analysis of the relationship between amino acids and BAs in the liver, it was found that tryptophan levels were positively correlated with dehydrocholic acid and glycocholic acid levels, suggesting that the reduction in these BAs due to the EBN intervention might also be related to changes in amino acids.

Discussion

Obesity, characterized by an excess accumulation of adipose tissue, significantly affects glucose and lipid metabolism. This study demonstrates that a high-dose EBN intervention effectively controls the increase in body weight and fat mass in obese mice. Furthermore, it improves lipid disorders, reduces inflammation, increases the concentration of sialic acid in LDL and decreases Ox-LDL levels. Consequently, EBN plays a pivotal role in addressing the metabolic imbalances related to glucose, lipids, and fat in the context of obesity. The upcoming discussion will integrate the findings from the colonic microbiota and liver and colonic transcriptomics and metabolomics to investigate how EBN reduces body fat, lowers blood sugar levels, decreases blood lipids, and ameliorates chronic inflam-

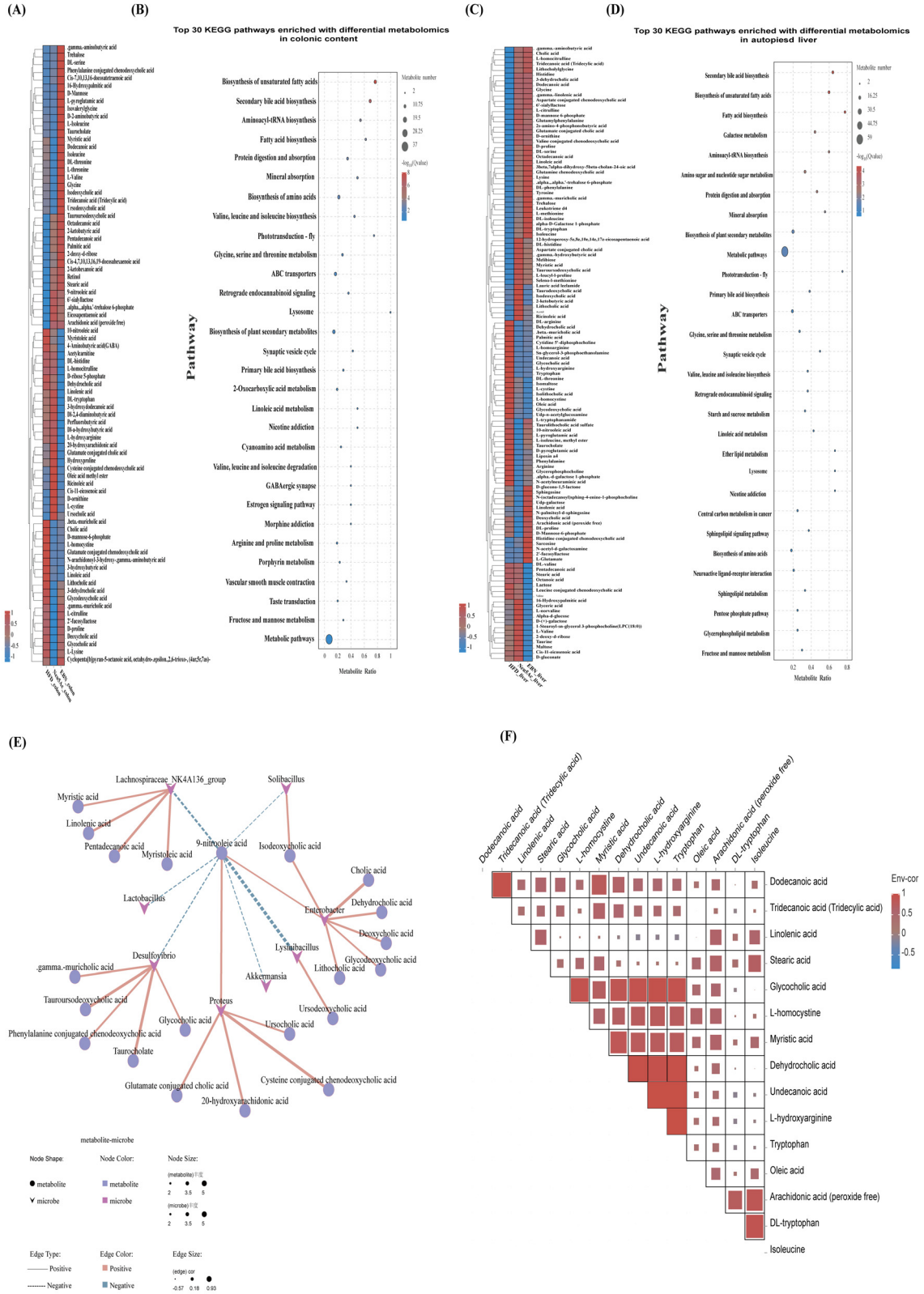

Fig. 6 Changes in metabolome expression in colonic contents and liver autopsied from 5 obese mice intervened by EBN post 10-week supplementation. (A and B) Metabolome expression in colonic contents: (A) comparison of differentially targeted metabolites related to glucose and lipid metabolism in colonic contents and (B) the top 30 KEGG pathways enriched with differentially targeted metabolites related to glucose and lipid metabolism in colon contents. (C and D) Metabolome expression in the liver: (C) comparison of differentially targeted metabolites related to glucose and lipid metabolism in the liver and (D) the top 30 KEGG pathways enriched with differentially targeted metabolites related to glucose and lipid metabolism in the liver. (E) Correlation network diagram between the gut microbiota and metabolites in colon contents. (F) Correlation heatmap of metabolites in the liver: fatty acids, amino acids, and bile acids.

mation in obese individuals. Anticipating the potential of EBN in regulating glucose and lipid metabolic disorders in obese mice, this study aims to provide a foundational framework for understanding the effectiveness of EBN in the context of chronic conditions.

The mechanism of lipid-lowering effects

In this study, mice were subjected to obesity induction using a high-fat diet. A comparative analysis between normal weight and obese mice revealed that the latter exhibited an amplified intake of food energy and a reduced level of physical activity, resulting in significant alterations in obesity-associated physiological markers. However, EBN intervention controlled body weight gain, reduced body fat in obese mice, and improved obesity-associated physiological markers induced by a high-fat diet. This suggests that EBN may disrupt the body's positive energy balance and cause disordered lipid metabolism within the body. It is speculated that this process can be accomplished through the following two pathways: EBN intervention may reduce lipid absorption and synthesis in the intestine and liver. The high-fat feed ingested by mice is broken down into fatty acids and glycerol. These components are then reabsorbed by the intestines and enter the bloodstream. Within liver cells, fatty acids are reassembled into TG or other lipid molecules.[28–30] EBN intervention affected genes related to lipid absorption and TC metabolism in the intestine, as well as lipid synthesis in the liver, including *Abca1*, *Fabp6*, *PLTP*, *PPAR*, *Lrp1*, *Ggt1*, *Cyp2C66*, *Cyp2c69*, *Pnlip*, *CLPS*, and *Elovl3*, and increased the abundance of gut microbes related to carbohydrate and fat metabolism and energy metabolic pathways, which may contribute to a decrease in blood TG, TC, and LDL levels, while simultaneously promoting an increase in HDL levels. The metabolomic results also indicated that mice subjected to EBN intervention exhibited an elevated concentration of fatty acids in the colonic content and a decrease in fatty acid content in the liver. Ultimately, EBN intervention could control weight gain and reduce body fat content in obese mice. It is worth highlighting that EBN intervention not only lowers plasma LDL levels but also demonstrates the capacity to elevate sialic acid content in LDL in the plasma while concurrently reducing Ox-LDL levels. Natural LDL is a cholesterol-rich lipoprotein with highly glycosylated surface proteins. Sialic acid is the main residue linked to Gal or GalNAc with α2-3 or α2-6 O-linked glycosidic bonds.[31] Natural LDL in the blood circulation does not cause lipid accumulation in the artery wall, whereas desialylated LDL (ds-LDL) is atherosclerotic and causes lipid deposition.[32–34] After losing sialic acid, LDL molecules easily oxidize to form Ox-LDL.[35] The study found that intervention with EBN can increase *B3gal5*, *Mgat4c*, and *Man1c1* in the liver and colon, which may increase the sialic acid load on LDL. This suggests that EBN intervention can also affect obesity-related lipid metabolism disorders by altering lipoprotein sialylation modifications.

EBN intervention may increase hepatic bile acid excretion and reduce intestinal secondary bile acid reflux. A high-fat diet leads to the increased reabsorption of bile acids in the intestines and the synthesis of bile acids in the liver, thereby promoting fat accumulation. At the same time, it reduces the abundance of some components of the gut microbiota that convert primary BAs into secondary BAs, increasing the abundance of aerobic, proinflammatory bacteria and bile acid modification-associated bacteria.[36] Subsequently, liver inflammation increases, thereby inhibiting bile acid transporters. Inflammation disrupts the gut barrier *via* STAT3 activation, leading to the loss of FXR function and the negative feedback regulation (FXR-FGf19) of bile acid synthesis,[37] potentially reducing GLP-1 secretion[38,39] and resulting in a reduced efficiency of energy metabolism, which in turn promotes fat accumulation and the development of obesity. The intervention with EBN could improve the gut microbiota by increasing the abundance of microbiota components positively related to secondary BAs and decreasing the abundance of microbiota components positively related to inflammation. It also influenced the transcriptome in the colon by decreasing the expression levels of *Ereg*, *Ntrk2*, *Tlr2*, *Thbs1*, *Ppara*, and *Cxcl12*, inhibiting the PI3K-Akt, PPAR and NF-κB signaling pathways; it then decreased serum IL-1β, IL-6 and TNF-α levels, while increased the serum GLP-1 level. The intervention with EBN also decreased the *Lrp1*, *Slc10a2*, and *Slc51a* expression levels in the colon, inhibiting chylomicron-remnant and BA transport to the liver, while it increased *Slc51a*, *Abcb1a*, and *Aqp4* expression levels in the liver and promoted BA transport to the colon, thereby promoting the excretion of combined bilirubin and enhancing bile flow. The outcomes obtained from metabolomic analysis further reveal a decline in the levels of BAs within the liver, while an increase in their levels is observed within the colon.

In summary, EBN intervention could potentially improve lipid metabolism and reduce body fat accumulation not only by enhancing the structure and function of the gut microbiome and influencing genes related to fat synthesis and absorption, thereby reducing fat absorption and synthesis, but also by ameliorating the variety of BAs and the state of metabolic imbalance during the development of obesity, which in turn could alleviate the chronic inflammatory state and improve lipid and energy metabolism in obese individuals.

The mechanism of lowering hyperglycemia effects

Compared to non-obese individuals, obese individuals exhibit higher fasting insulin levels and greater insulin resistance.[40,41] Additionally, glucose tolerance is impaired following an oral glucose load in obese individuals.[42] This study has revealed that EBN intervention regulated elevated FBG, reduced fasting INS levels, and lowered the HOMA-IR value in obese mice, thereby alleviating impaired glucose tolerance. By further integrating transcriptional and metabolomic changes, this study explored the potential mechanisms by which EBN intervention controls elevated blood glucose levels and improves glucose tolerance in obese mice. This process may occur through the following three pathways: EBN reduces body fat, regulates the adipocytokine signaling pathway, and improves insulin resistance. Body fat, particularly visceral fat, significantly increases

glucose metabolism and insulin resistance in the liver and peripheral tissues, leading to insulin resistance and an increased risk of diabetes.[43,44] EBN intervention may reduce the visceral fat content by decreasing lipid absorption and synthesis and by improving the bile acid balance *via* the gut–liver axis. This, in turn, affects the signaling pathways of adipocytes in the liver, reduces the enhancement of hepatic glucose utilization, increases the expression levels of genes related to glycogen synthesis, and leads to a reduction in monosaccharides and an increase in polysaccharides in hepatic metabolites. This suggests that controlling the liver fat content is beneficial for the regulation of blood sugar levels in the body. The proinflammatory cytokine TNF-α has been implicated as a link between obesity and insulin resistance.[45] TNF-α interferes with the early steps of insulin signaling. Several studies have shown that TNF-α inhibits IRS1 tyrosine phosphorylation by promoting serine phosphorylation. In obesity, the production of TNF-α by macrophages and other immune cells within the adipose tissue increases, leading to an inflammatory response in the fat tissue. EBN supplementation reduced the amount of visceral fat, decreased the secretion of TNF-α from excess adipose tissue, and alleviated insulin resistance.

EBN improved the gut microbiota of mice, alleviated oxidative stress in the liver through the gut–liver axis, and reduced the levels of chronic inflammatory markers in the serum, thereby enhancing insulin sensitivity and the body's ability to regulate blood glucose. Dysbiosis, which is an imbalance in the gut microbiota, can impair the development of gut-associated lymphoid tissue and compromise the integrity of the intestinal barrier. This leads to increased intestinal permeability, allowing pathogenic components, such as lipopolysaccharides (LPS) and trimethylamine (TMA), to enter the bloodstream, activating inflammatory pathways, such as nuclear factor (NF)-κB and activator protein (AP)-1, resulting in the upregulation of pro-inflammatory cytokines, causing chronic low-grade inflammation and interfering with the action of insulin.[46–48] Simultaneously, TMA is oxidized in the liver by the action of the Fmo3 enzyme to form TMAO, which can induce oxidative stress and inflammation in the liver and reduce the body's glycemic regulation ability.[49,50] This study found that EBN intervention improved the composition of the gut microbiota in obese mice, inhibited the LPS biosynthesis pathways of the gut microbiota, and decreased immune-inflammatory signaling pathways in the colonic mucosa and liver, thereby reducing the levels of markers of inflammation (IL-1β, IL-6, and TNF-α), alleviating the state of chronic inflammation and improving body insulin sensitivity. Simultaneously, it decreased hepatic *Fmo3* transcription levels and TMAO levels, reduced oxidative stress in the liver and enhanced glycemic regulation in mice.

EBN influenced the circadian rhythm and improved insulin function. Physiological rhythm is a regular pattern of physiological and behavioral changes that organisms undergo within a 24-hour cycle. It plays a crucial role in regulating metabolism and energy balance, including appetite, insulin sensitivity, and glucose metabolism, all of which are regulated by the daily biological clock, aiding adaptation to energy demands at different times of the day.[51] This cyclical variation is regulated by the internal biological clock within an organism.[52] The rhythmicity of *clock*, *bmal1*, and *per2* gene expression is significantly dampened in the liver and white adipose tissue among the mice on a high-fat diet.[53] In the present study, we observed reduced expression levels of *clock* and *npas2* mRNA and increased expression levels of *bmal1*, *per1* and *per2* mRNA in the liver in the EBN group, which may have promoted the upregulation of insulin secretion by β-cells and the postprandial enteric insulin GLP-1 response by L-cells.[54–56] This study also noted that serum GLP-1 levels were elevated in the EBN group mice (*vs.* HFD, $P < 0.05$). Previous studies have shown that increased GLP-1 levels contribute to improved glucose control in obese individuals.[57–59] This suggests that EBN intervention influences physiological rhythms, which may help control elevated blood glucose in individuals with obesity induced by a high-fat diet.

Limitations

This study investigated the effects of EBN intervention on dysregulated glucose and lipid metabolism using a high-fat obesity animal model and explored the potential mechanisms through transcriptional and metabolomic analyses. However, EBN contains a series of bioactive components that vary depending on the origin of the raw materials, different production conditions and batches, and other factors. The bioactive substances detected in the bird's nest product used in our experiment included polysialic acid, water-soluble small molecule bird's nest protein, glutathione, and epidermal growth factor. Among these active components, only polysialic acid has been measured at >360 mg/100 g, while the contents of the other active components within this EBN have not been fully determined. This study focused solely on the EBN products processed using a particular technique and did not compare those processed using other methods. The efficacy of this type of EBN also needs to be validated in population trials. Additionally, aside from sialic acid, the identification of other potential bioactive components in EBN remains unclear and requires further exploration, and further attention can also be paid to the effects of EBN on cellular or molecular sialylation modification.

Conclusions

EBN has the potential to regulate glucose and lipid metabolic disorders *via* the gut–liver axis in obese mice. EBN can enhance the gut microbiota and intestinal immunity, relieve chronic inflammation levels in serum, improve the antioxidant capacity and circadian rhythm in the liver, promote bile acid metabolism and decrease lipid absorption and lipid synthesis *via* the gut–liver axis, thus reducing blood lipid and fat accumulation as well as improving islet function, which lowers blood glucose levels.

Author contributions

All authors contributed to the study conception and design. ZW, HWL, XYW, and QF conceived and designed the experiments. ZW, ZMZ, KD, YCZ, LXZ, and YPL performed the experiments. ZW, ZMZ, XYW, and QF analyzed the data. ZMZ, XCL, MYQ, KD, YCZ, LXZ, and YPL contributed to reagents/materials/analysis tools. ZW, HWL, and QF wrote the paper. All authors have read and approved the final manuscript.

Ethics approval

All experimental procedures were performed according to the guidelines of the Institutional Animal Care and Use Committee of Laboratory Animal Center of Xiamen University and followed the International Association of Veterinary Editors guidelines for the Care and Use of Laboratory Animals. The animal use protocol has been reviewed and approved by the Animal Ethical and Welfare Committee of Laboratory Animal Center of Xiamen University, approval no. XMULAC20200185.

Data availability

The raw sequencing data from this study have been deposited in the Genome Sequence Archive[60] at the BIG Data Center (**https://bigd.big.ac.cn**), Beijing Institute of Genomics (BIG), Chinese Academy of Sciences,[61] under the accession numbers CRA014672 and CRA014673. The data can be accessed at the following links: **https://ngdc.cncb.ac.cn/gsa/s/5rT88YWZ** and **https://ngdc.cncb.ac.cn/gsa/s/RyGE660B**.

Conflicts of interest

The authors declare that they have no competing interests.

Acknowledgements

This research is supported by the Incubation Fund of Zhongshan Hospital, Fudan University (Xiamen Branch) (No. 2020ZSXMYS24). The funders had no role in study design, data collection and analysis, decision to publish, or preparation of the manuscript.

References

1 S. Kumanyika and W. H. Dietz, Solving Population-wide Obesity - Progress and Future Prospects, *N. Engl. J. Med.*, 2020, **383**, 2197–2200.
2 R. Ruze, T. Liu, X. Zou, J. Song, Y. Chen, R. Xu, X. Yin and Q. Xu, Obesity and type 2 diabetes mellitus: connections in epidemiology, pathogenesis, and treatments, *Front. Endocrinol.*, 2023, **14**, 1161521.
3 M. E. Piché, A. Tchernof and J. P. Després, Obesity Phenotypes, Diabetes, and Cardiovascular Diseases, *Circ. Res.*, 2020, **126**, 1477–1500.
4 . W. O. F. World obesity atlas 2022. (London: World Obesity Federation) (2022). *Journal*.
5 M. Versini, P. Y. Jeandel, E. Rosenthal and Y. Shoenfeld, Obesity in autoimmune diseases: not a passive bystander, *Autoimmun. Rev.*, 2014, **13**, 981–1000.
6 T. V. Rohm, D. T. Meier, J. M. Olefsky and M. Y. Donath, Inflammation in obesity, diabetes, and related disorders, *Immunity*, 2022, **55**, 31–55.
7 Y. Zhang, J. R. Sowers and J. Ren, Targeting autophagy in obesity: from pathophysiology to management, *Nat. Rev. Endocrinol.*, 2018, **14**, 356–376.
8 G. I. Shulman, Ectopic fat in insulin resistance, dyslipidemia, and cardiometabolic disease, *N. Engl. J. Med.*, 2014, **371**, 2237–2238.
9 K. Sun, C. M. Kusminski and P. E. Scherer, Adipose tissue remodeling and obesity, *J. Clin. Invest.*, 2011, **121**, 2094–2101.
10 R. H. Lustig, Processed Food-An Experiment That Failed, *JAMA Pediatr.*, 2017, **171**, 212–214.
11 G. Li, T. H. Lee, G. Chan and K. W. K. Tsim, Editorial: Edible Bird's Nest-Chemical Composition and Potential Health Efficacy and Risks, *Front. Pharmacol.*, 2021, **12**, 819461.
12 M. Yuan, X. Lin, D. Wang and J. Dai, Proteins: Neglected active ingredients in edible bird's nest, *Chin. Herb. Med.*, 2023, **15**, 383–390.
13 K. C. Chok, M. G. Ng, K. Y. Ng, R. Y. Koh, Y. L. Tiong and S. M. Chye, Edible Bird's Nest: Recent Updates and Industry Insights Based On Laboratory Findings, *Front. Pharmacol.*, 2021, **12**, 746656.
14 T. H. Lee, W. A. Wani, C. H. Lee, K. K. Cheng, S. Shreaz, S. Wong, N. Hamdan and N. A. Azmi, Edible Bird's Nest: The Functional Values of the Prized Animal-Based Bioproduct From Southeast Asia-A Review, *Front. Pharmacol.*, 2021, **12**, 626233.
15 Y. Zhang, H. Al-Shuwayah, M. Ismail and M. Umar Imam, Edible Bird's Nest Regulates Hepatic Cholesterol Metabolism through Transcriptional Regulation of Cholesterol Related Genes, *J. Evidence-Based Complementary Altern. Med.*, 2022, **2022**, 1–10.
16 J. Shi, X. Hu, X. Zou, J. Zhao, W. Zhang, M. Holmes, X. Huang, Y. Zhu, Z. Li, T. Shen and X. Zhang, A rapid and nondestructive method to determine the distribution map of protein, carbohydrate and sialic acid on Edible bird's nest by hyper-spectral imaging and chemometrics, *Food Chem.*, 2017, **229**, 235–241.
17 B. Wang, Molecular mechanism underlying sialic acid as an essential nutrient for brain development and cognition, *Adv. Nutr.*, 2012, **3**, 465s–472s.
18 R. Schauer, Sialic acids: fascinating sugars in higher animals and man, *Zoology*, 2004, **107**, 49–64.

19 S. D. Guo, H. Tian, R. R. Dong, N. N. Yang, Y. Zhang, S. T. Yao, Y. J. Li, Y. W. Zhou, Y. H. Si and S. C. Qin, Exogenous supplement of N-acetylneuraminic acid ameliorates atherosclerosis in apolipoprotein E-deficient mice, *Atherosclerosis*, 2016, **251**, 183–191.

20 S. Abdul Babji and N. Aliah Daud, *Swiftlet's Nest as Potential Prebiotic Compound for the Gut Beneficial Bacteria*, Brawijaya University, 2021, vol. 16, pp. 1–10.

21 D. Aliah, S. Razid Sarbini, A. Salam Babji, S. Mohamad Yusop and S. Joe Lim, Characterization of edible swiftlet's nest as a prebiotic ingredient using a simulated colon model, *Ann. Microbiol.*, 2019, **68**, 1235–1246.

22 R. Zhao, X. J. Kong, G. LI, X. Q. Yin, C. P. Fang and X. P. Lai, Influence of Edible Bird′s Nest on Enteric Bacteria Flora of Mice, *Prog. Vet. Med.*, 2014, **35**, 86–89.

23 Z. Han-ying, L. Hui, Z. Ying-ying and L. Hong-wei, Effects of Bifidobacterium CP-9 and Lactobacillus Reuteri on Glucose and Lipid Metabolism in Obese Mice %J, *J. Nutr.*, 2021, **43**, 283–288.

24 . A. o. t. S. A. f. M. Regulation, National Health Commission, and State Administration of Traditional Chinese Medicine on the Release of the Catalogue of Nutrient Supplements for Health Food Raw Materials (2020 Edition) and the Catalogue of Nutrient Supplements for Health Functions Permitted by Health Food Claims (2020 Edition). *Journal*.

25 A. I. Mina, R. A. LeClair, K. B. LeClair, D. E. Cohen, L. Lantier and A. S. Banks, CalR: A Web-Based Analysis Tool for Indirect Calorimetry Experiments, *Cell Metab.*, 2018, **28**, 656–666.

26 E. J. Want, P. Masson, F. Michopoulos, I. D. Wilson, G. Theodoridis, R. S. Plumb, J. Shockcor, N. Loftus, E. Holmes and J. K. Nicholson, Global metabolic profiling of animal and human tissues via UPLC-MS, *Nat. Protoc.*, 2013, **8**, 17–32.

27 C. H. Zhu, Y. X. Li, Y. C. Xu, N. N. Wang, Q. J. Yan and Z. Q. Jiang, Tamarind Xyloglucan Oligosaccharides Attenuate Metabolic Disorders via the Gut-Liver Axis in Mice with High-Fat-Diet-Induced Obesity, *Foods*, 2023, **12**, 1382.

28 H. R. Davis Jr., L. J. Zhu, L. M. Hoos, G. Tetzloff, M. Maguire, J. Liu, X. Yao, S. P. Iyer, M. H. Lam, E. G. Lund, P. A. Detmers, M. P. Graziano and S. W. Altmann, Niemann-Pick C1 Like 1 (NPC1L1) is the intestinal phytosterol and cholesterol transporter and a key modulator of whole-body cholesterol homeostasis, *J. Biol. Chem.*, 2004, **279**, 33586–33592.

29 B. Klop, J. Wouter Jukema, T. J. Rabelink and M. Castro Cabezas, A physician's guide for the management of hypertriglyceridemia: the etiology of hypertriglyceridemia determines treatment strategy, *Panminerva Med.*, 2012, **54**, 91–103.

30 B. Klop, J. W. Elte and M. C. Cabezas, Dyslipidemia in obesity: mechanisms and potential targets, *Nutrients*, 2013, **5**, 1218–1240.

31 V. V. Tertov and A. N. Orekhov, Metabolism of native and naturally occurring multiple modified low density lipoprotein in smooth muscle cells of human aortic intima, *Exp. Mol. Pathol.*, 1997, **64**, 127–145.

32 A. Ruelland, G. Gallou, B. Legras, F. Paillard and L. Cloarec, LDL sialic acid content in patients with coronary artery disease, *Clin. Chim. Acta*, 1993, **221**, 127–133.

33 E. R. Zakiev, V. N. Sukhorukov, A. A. Melnichenko, I. A. Sobenin, E. A. Ivanova and A. N. Orekhov, Lipid composition of circulating multiple-modified low density lipoprotein, *Lipids Health Dis.*, 2016, **15**, 134.

34 V. I. Summerhill, A. V. Grechko, S. F. Yet, I. A. Sobenin and A. N. Orekhov, The Atherogenic Role of Circulating Modified Lipids in Atherosclerosis, *Int. J. Mol. Sci.*, 2019, **20**, 3561.

35 M. L. J. Jeurissen, S. M. A. Walenbergh, T. Houben, M. J. J. Gijbels, J. Li, T. Hendrikx, Y. Oligschlaeger, P. J. van Gorp, C. J. Binder, M. Donners and R. Shiri-Sverdlov, Prevention of oxLDL uptake leads to decreased atherosclerosis in hematopoietic NPC1-deficient Ldlr(-/-) mice, *Atherosclerosis*, 2016, **255**, 59–65.

36 A. Wahlström, S. I. Sayin, H. U. Marschall and F. Bäckhed, Intestinal Crosstalk between Bile Acids and Microbiota and Its Impact on Host Metabolism, *Cell Metab.*, 2016, **24**, 41–50.

37 X. Zheng, T. Chen, R. Jiang, A. Zhao, Q. Wu, J. Kuang, D. Sun, Z. Ren, M. Li, M. Zhao, S. Wang, Y. Bao, H. Li, C. Hu, B. Dong, D. Li, J. Wu, J. Xia, X. Wang, K. Lan, C. Rajani, G. Xie, A. Lu, W. Jia, C. Jiang and W. Jia, Hyocholic acid species improve glucose homeostasis through a distinct TGR5 and FXR signaling mechanism, *Cell Metab.*, 2021, **33**, 791–803.

38 C. D. Fuchs and M. Trauner, Role of bile acids and their receptors in gastrointestinal and hepatic pathophysiology, *Nat. Rev. Gastroenterol. Hepatol.*, 2022, **19**, 432–450.

39 V. L. Albaugh, B. Banan, J. Antoun, Y. Xiong, Y. Guo, J. Ping, M. Alikhan, B. A. Clements, N. N. Abumrad and C. R. Flynn, Role of Bile Acids and GLP-1 in Mediating the Metabolic Improvements of Bariatric Surgery, *Gastroenterology*, 2019, **156**, 1041–1051.

40 Q. Huang, X. Zou, P. Gao, X. Han, X. Zhou and L. Ji, How does obesity affect mortality through blood pressure and blood glucose in Chinese and US citizens? Insights from a causal mediation analysis of two large cohorts, *J. Glob. Health*, 2023, **13**, 04032.

41 M. R. Saraswati, I. B. A. Nugraha and K. Suastika, Similar Blood Glucose Pattern with Highest Peak at Minute 45 on Oral Glucose Tolerance Test Despite Higher Fasting Insulin and Insulin Resistance in Healthy Obese than Non-Obese Subject, *Acta Med. Indones.*, 2022, **54**, 210–217.

42 H. Wang, M. Wang, J. Wang, H. Liu, R. Lu, T. Duan, X. Gong, S. Feng, Z. Cui, Y. Liu, C. Li and J. Ma, Cost-effectiveness analysis of comprehensive intervention programs to control blood glucose in overweight and obese type 2 diabetes mellitus patients based on a real-world setting: Markov modeling, *Ann. Transl. Med.*, 2019, **7**, 676.

43 J. Zhang and F. Liu, Tissue-specific insulin signaling in the regulation of metabolism and aging, *IUBMB Life*, 2014, **66**, 485–495.
44 A. N. Peiris, M. F. Struve, R. A. Mueller, M. B. Lee and A. H. Kissebah, Glucose metabolism in obesity: influence of body fat distribution, *J. Clin. Endocrinol. Metab.*, 1988, **67**, 760–767.
45 X. Guo, C. Li, J. Wu, Q. Mei, C. Liu, W. Sun, L. Xu and S. Fu, The association of TNF-α -308G/A and -238G/A polymorphisms with type 2 diabetes mellitus: a meta-analysis, *Biosci. Rep.*, 2019, **39**, BSR20191301.
46 T. P. M. Scheithauer, E. Rampanelli, M. Nieuwdorp, B. A. Vallance, C. B. Verchere, D. H. van Raalte and H. Herrema, Gut Microbiota as a Trigger for Metabolic Inflammation in Obesity and Type 2 Diabetes, *Front. Immunol.*, 2020, **11**, 571731.
47 H. Yuan, Y. Li, F. Ling, Y. Guan, D. Zhang, Q. Zhu, J. Liu, Y. Wu and Y. Niu, The phytochemical epigallocatechin gallate prolongs the lifespan by improving lipid metabolism, reducing inflammation and oxidative stress in high-fat diet-fed obese rats, *Aging Cell*, 2020, **19**, e13199.
48 A. I. Legaki, Moustakas II, M. Sikorska, G. Papadopoulos, R. I. Velliou and A. Chatzigeorgiou, Hepatocyte Mitochondrial Dynamics and Bioenergetics in Obesity-Related Non-Alcoholic Fatty Liver Disease, *Curr. Obes. Rep.*, 2022, **11**, 126–143.
49 F. Nian, C. Zhu, N. Jin, Q. Xia, L. Wu and X. Lu, Gut microbiota metabolite TMAO promoted lipid deposition and fibrosis process via KRT17 in fatty liver cells in vitro, *Biochem. Biophys. Res. Commun.*, 2023, **669**, 134–142.
50 D. Vukićević, B. Rovčanin, K. Gopčević, S. Stanković, D. Vučević, B. Jorgačević, D. Mladenović, M. Vesković, J. Samardžić, R. Ješić and T. Radosavljević, The Role of MIF in Hepatic Function, Oxidative Stress, and Inflammation in Thioacetamide-induced Liver Injury in Mice: Protective Effects of Betaine, *Curr. Med. Chem.*, 2021, **28**, 3249–3268.
51 X. Pan, S. Mota and B. Zhang, Circadian Clock Regulation on Lipid Metabolism and Metabolic Diseases, *Adv. Exp. Med. Biol.*, 2020, **1276**, 53–66.
52 D. Jakubowicz, R. C. Rosenblum, J. Wainstein and O. Twito, Influence of Fasting until Noon (Extended Postabsorptive State) on Clock Gene mRNA Expression and Regulation of Body Weight and Glucose Metabolism, *Int. J. Mol. Sci.*, 2023, **24**, 7154.
53 L. N. Woodie, K. T. Oral, B. M. Krusen and M. A. Lazar, The Circadian Regulation of Nutrient Metabolism in Diet-Induced Obesity and Metabolic Disease, *Nutrients*, 2022, **14**, 3136.
54 E. Vieira, T. P. Burris and I. Quesada, Clock genes, pancreatic function, and diabetes, *Trends Mol. Med.*, 2014, **20**, 685–693.
55 B. Marcheva, K. M. Ramsey, E. D. Buhr, Y. Kobayashi, H. Su, C. H. Ko, G. Ivanova, C. Omura, S. Mo, M. H. Vitaterna, J. P. Lopez, L. H. Philipson, C. A. Bradfield, S. D. Crosby, L. JeBailey, X. Wang, J. S. Takahashi and J. Bass, Disruption of the clock components CLOCK and BMAL1 leads to hypoinsulinaemia and diabetes, *Nature*, 2010, **466**, 627–631.
56 D. Jakubowicz, J. Wainstein, S. Tsameret and Z. Landau, Role of High Energy Breakfast "Big Breakfast Diet" in Clock Gene Regulation of Postprandial Hyperglycemia and Weight Loss in Type 2 Diabetes, *Nutrients*, 2021, **13**, 1558.
57 W. Wang, R. Wei, Z. Huang, J. Luo, Q. Pan and L. Guo, Effects of treatment with Glucagon-like peptide-1 receptor agonist on prediabetes with overweight/obesity: A systematic review and meta-analysis, *Diabetes Metab. Res. Rev.*, 2023, **39**, e3680.
58 T. Hira, A. Trakooncharoenvit, H. Taguchi and H. Hara, Improvement of Glucose Tolerance by Food Factors Having Glucagon-Like Peptide-1 Releasing Activity, *Int. J. Mol. Sci.*, 2021, **22**, 6623.
59 S. Suzuki and S. Aoe, High β-Glucan Barley Supplementation Improves Glucose Tolerance by Increasing GLP-1 Secretion in Diet-Induced Obesity Mice, *Nutrients*, 2021, **13**, 527.
60 T. Chen, X. Chen, S. Zhang, J. Zhu, B. Tang, A. Wang, L. Dong, Z. Zhang, C. Yu, Y. Sun, L. Chi, H. Chen, S. Zhai, Y. Sun, L. Lan, X. Zhang, J. Xiao, Y. Bao, Y. Wang, Z. Zhang and W. Zhao, The Genome Sequence Archive Family: Toward Explosive Data Growth and Diverse Data Types, *Genomics, Proteomics Bioinf.*, 2021, **19**, 578–583.
61 CNCB-NGDC Members and Partners, Database Resources of the National Genomics Data Center, China National Center for Bioinformation in 2022, *Nucleic Acids Res.*, 2022, 50, D27–D38.